# Dynamics of a discotic liquid crystal in the isotropic phase

Jie Li, Kendall Fruchey, and M. D. Fayer[a)]
*Department of Chemistry, Stanford University, Stanford, California 94305*

(Received 9 August 2006; accepted 5 October 2006; published online 15 November 2006)

Optically heterodyne-detected optical Kerr effect (OHD-OKE) experiments are conducted to study the orientational dynamics of a discotic liquid crystal 2,3,6,7,10,11-hexakis(pentyloxy)triphenylene (HPT) in the isotropic phase near the columnar-isotropic (*C-I*) phase transition. The OHD-OKE signal of HPT is characterized by an intermediate power law $t^{-0.76\pm0.02}$ at short times (a few picoseconds), a von Schweidler power law $t^{-0.26\pm0.01}$ at intermediate times (hundreds of picoseconds), and an exponential decay at long times (tens of nanoseconds). The exponential decay has Arrhenius temperature dependence. The functional form of the total time dependent decay is identical to the one observed previously for a large number of molecular supercooled liquids. The mode coupling theory schematic model based on the Sjögren [Phys. Rev. A **33**, 1254 (1986)] model is able to reproduce the HPT data over a wide range of times from $<1$ ps to tens of nanoseconds. The studies indicate that the HPT *C-I* phase transition is a strong first order transition, and the dynamics in the isotropic phase display a complex time dependent profile that is common to other molecular liquids that lack mesoscopic structure. © *2006 American Institute of Physics*. [DOI: 10.1063/1.2378623]

## I. INTRODUCTION

Since the discovery of the first discotic liquid crystal in 1977,[1] there has been growing interest in the mesophases formed by disklike molecules. Usually these molecules consist of a rigid aromatic core with several flexible aliphatic chains bound to the edges. Two types of mesophases, nematic and columnar, are typically formed by disklike molecules. In the discotic nematic phase, the normals to the disks are on average aligned along a common direction, the macroscopic director, and there is no long-range positional order. This structure is quite similar to the nematic structure found in rodlike mesogens. In another type of arrangement, discogens stack on top of each other to form columns, which then self-organize into a two-dimensional lattice. This type of order is referred to as a columnar phase. These different types of molecular ordering give rise to interesting dynamical properties, and the phase transitions between the variety of mesophases and the isotropic liquid phase are often rich in features. The nature of discotic liquid crystals is interesting at a fundamental level and technologically important.

Here we present a study of the dynamics of a typical discotic liquid crystal 2,3,6,7,10,11-hexakis(pentyloxy)-triphenylene (HPT) in the isotropic phase using time domain optical heterodyne-detected optical Kerr effect (OHD-OKE) experiments. Neat HPT has a columnar-isotropic (*C-I*) transition at 395 K. X-ray diffraction patterns [2,3] of the mesophase indicate a two-dimensional hexagonal lattice with an intercolumnar spacing of 19.8 Å. The stacking of the discogens within each column has one-dimensional positional ordering with spacing of 3.6 Å, and there is no correlation between the positions of molecules from different columns. The orientational order parameter, measured with Fourier transform infrared (FTIR), was found to change discontinuously across the *C-I* phase transition.[4] Dynamical properties in the hexagonal columnar phase formed by HPT and other mesogens have been studied using dielectric spectroscopy,[5,6] neutron scattering,[7] molecular dynamics simulations,[8] and NMR.[9–12] In some of these studies, the dynamics in isotropic liquid phase were also addressed and compared to those of columnar phase.

The current work addresses the temperature dependent dynamical features of the orientational relaxation process in the isotropic phase. The results are discussed with a comparison to two other types of liquid systems previously studied using the identical technique: rodlike nematogens in the isotropic phase[13–17] and supercooled liquids.[15,18–22] The experiments presented here are conducted in the neighborhood of the *C-I* phase transition because this is the region where differences and similarities in the comparison between columnar liquid crystals and nematic liquid crystals would be expected to be most apparent. Nematogens also have a structural phase transition, the nematic-isotropic (*N-I*) transition.[23] The dynamics of nematogens in the isotropic phase are strongly influenced by local structures (pseudonematic domains) with a correlation length increasing dramatically as the phase transition is approached.[23] This pretransitional effect has been confirmed many times for rodlike nematogens using different techniques[23] and for a discotic nematogen[24] as well. A recent computer simulation study[25] performed on a variety of model systems including rodlike and disklike nematogens revealed universal power law regimes on short to intermediate time scales as these systems cross *N-I* phase transition. In explaining these phenomena, large fluctuation of orientational order parameter near the phase transition is believed to play an important role.[23–25] In contrast, supercooled liquids do not have a structural phase

[a)]Electronic mail: fayer@stanford.edu

 

transition. The nature of the dynamical slowing down that occurs as a supercooled liquid passes through the glass transition is still a subject under debate.

Although the microscopic mechanisms underlying the dynamics of supercooled liquids and nematogens in the isotropic phase are fundamentally different, seven supercooled liquids and six nematogens in the isotropic phase[13,15,20] have been shown to display the same functional form of the OHD-OKE decays over a wide range of times and temperatures. Both types of systems display two power laws on the short to intermediate time scales followed by an exponential decay on the longest time scale. There are some major differences as well. The values of the exponents in the power laws fall into two categories. Furthermore, the long time scale exponential relaxation displays different temperature dependences. The differences are related to the distinct physics of the phase transitions the two types of systems undergo.

A mode coupling theory approach[26,27] has the potential to describe the critical properties of supercooled liquids by properly taking into account the memory effects at low temperatures. A schematic mode coupling model was developed to describe the OHD-OKE experiments on supercooled liquids,[28] and it has been applied with considerable success.[20,28] A modified form of the schematic mode coupling theory (MCT) was developed and successfully applied to the OHD-OKE experimental results on nematogens in the isotropic phase.[29]

The experimental results obtained here over a wide range of time scales (picoseconds to many tens of nanoseconds) and temperatures show that the discotic liquid crystal HPT in its isotropic phase exhibits OHD-OKE decays of the same functional form as nematogens in their isotropic phase and supercooled liquids.[20,28] The data are fit with the schematic MCT that was used to describe the dynamics of supercooled liquids. The agreement is excellent. The augmented schematic MCT used in the study of the isotropic phase of nematogens, which takes into account the isotropic-nematic phase transition,[29] was not necessary to reproduce the discotic isotropic phase dynamics. The net result is that HPT in its isotropic phase approaching the *C-I* phase transition behaves more like a normal liquid far from its glass transition than it does like a nematogen in the isotropic phase approaching the *N-I* phase transition.

## II. EXPERIMENTAL PROCEDURES

OHD-OKE spectroscopy[30–32] was used to study the orientational dynamics of a discotic liquid crystal HPT at various temperatures in the isotropic phase. The OHD-OKE experiment measures the time derivative of the polarizability-polarizability (orientational) correlation function, which is directly related to the data obtained from depolarized light scattering experiments by Fourier transform.[33–36] The polarizability-polarizability correlation function is essentially the second Legendre polynomial orientational correlation function except at short time (probably less than a few picoseconds) where collision induced effects (density fluctuations) can also contribute to the decay.[34–37] In the experiments, a pump pulse creates an orientational anisotropy and a probe pulse is used to heterodyne detect its decay at variable time delays. To observe the full range of liquid dynamics, at each temperature several sets of experiments were performed with different pulse lengths and delays. For times $t<30$ ns, a 5 kHz mode-locked Ti:sapphire laser/regenerative amplifier system was used ($\lambda=800$ nm) for both pump and probe. The pulse length was varied from 75 fs to 100 ps as the time scale of the measurement increased to improve the signal-to-noise ratio. For longer times, a cw diode laser was used as the probe, and a fast digitizer (1 ns per point) recorded the data. The scans taken over various time ranges overlapped substantially, permitting the data sets to be merged by adjusting only their relative amplitudes. The details of the experimental setup can be found in previously published work.[16,19]

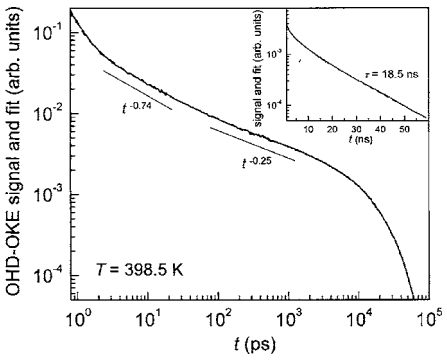


FIG. 1. OHD-OKE data for HPT at $T=398.5$ K. The dashed lines through the data are a fit using Eq. (1). The two straight lines are aids to the eyes indicating the intermediate power law (shorter time) and the von Schweidler power law (longer time). The inset shows the exponential decay at long times on a semilogarithmic scale.

HPT was purchased from Wako Chemicals USA, Inc. and was used without further purification other than filtration through 0.1 $\mu$m disk filters to remove dust and reduce light scattering. The sample was sealed under vacuum in a glass cuvette of optical path length of 1 cm. The cuvette was held in a liquid nitrogen constant flow cryostat where the temperature was controlled to $\pm 0.1$ K. Differential scanning calorimetry detected a feature, interpreted as the glass transition, at 216 K in the heating curve of rate=15 K/min.

## III. RESULTS AND DISCUSSION

Figure 1 shows a typical OHD-OKE decay curve for HPT in the isotropic phase. The data were taken at $T=398.5$ K. At times longer than 16 ns the decay is purely exponential, which appears as a straight line on a semilog plot (see inset). At short to intermediate time scales, the decay is complex and has a highly nonexponential character. The shape of the decay curve is very similar to that observed earlier for supercooled liquids and nematogens in the isotropic phase using the identical technique.[13,15] A phenomenological fitting function was applied extensively to model the decay curves in these different types of liquid systems. It was shown that this function provides an excellent global fit to the data over a wide time window from subpicoseconds to hundreds of nanoseconds. It is used to extract parameters that can be compared from one temperature to another and be-

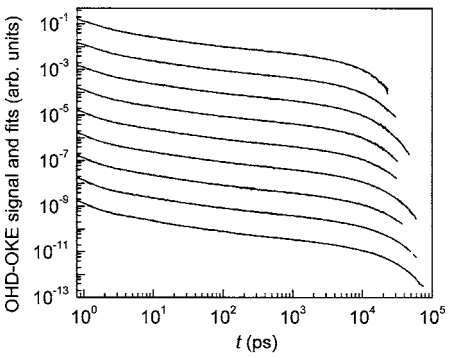


FIG. 2. Temperature dependent OHD-OKE data on a log plot. The data sets have been offset along the vertical axis for clarity of presentation. Fits to the data using Eq. (1) are also shown (dashed lines). The fit curves follow the experimental data very well and they are hardly discernible from the data. From top to bottom, the temperatures are 416, 413.5, 411, 408.5, 406, 403.5, 401, 398.5, and 396 K.

tween different liquids. The relationship of the empirical function to MCT has been discussed recently.[38] Here the HPT data are analyzed using the same fitting function[13,15]

$$F(t) = [at^{-s} + pt^{-z} + dt^{b-1}]\exp(-t/\tau). \quad (1)$$

The term $at^{-s}$ is used to model the steep decay at the shortest time scale from subpicoseconds to a few picoseconds. (In supercooled liquids the signal is often dominated by the intramolecular vibrational modes on this time scale, so the term $at^{-s}$ was not included and the data were fit on longer time scales.) $pt^{-z}$ describes the intermediate power law following the shortest time scale decay, and $dt^{b-1}$ is the power law that occurs just prior to the crossover to the final exponential decay. In supercooled liquids, this longest time scale power law is called the von Schweidler power law and the final exponential relaxation is referred to as the $\alpha$ relaxation. The calculated curve using Eq. (1) is shown as a dashed line on Fig. 1. It is virtually indistinguishable from the data over the full time window from 0.8 ps to 60 ns. Although there are a substantial number of parameters, the distinct behavior that occurs on widely separated time scales makes the fit robust. The fitting results for the data at 398.5 K are $s=3.17$, $z=0.74$, $b=0.75$, and $\tau_\alpha=18.6$ ns. In the double-logarithmic representation of Fig. 1, two straight lines are drawn as aides to the eyes indicating the two power laws $t^{-0.74}$ and $t^{-0.25}$. These two power laws span significant time intervals, but there is a large time range in the middle during which they overlap. A global fit is necessary to accurately extract the values of the exponents as one type of decay gives way to the next with increasing time scale. It is important to note again that the OHD-OKE experiment measures the time derivative of the polarizability-polarizability correlation function. Therefore, the intermediate power law is close to a logarithmic decay of the correlation function.

Figure 2 displays the temperature dependent OHD-OKE data for HPT. The curves have been offset along the vertical axis for clarity of presentation. From the top to the bottom, the curves are arranged in the order of decreasing temperatures. The temperatures are given in the figure caption. A global fit using Eq. (1) was performed for each temperature to examine quantitatively the temperature dependence of different components in the complex profile. The fits are the dashed curves, which are barely distinguishable from the data. All fits start from 0.8 ps. Data at shorter times are not under consideration because they are obscured by the electronic nonresonant response of the liquid, which is so strong that even with short pulses it still overwhelms the nuclear contributions to the signal. Equation (1) provides excellent fits to the data over the full time window at all temperatures studied.

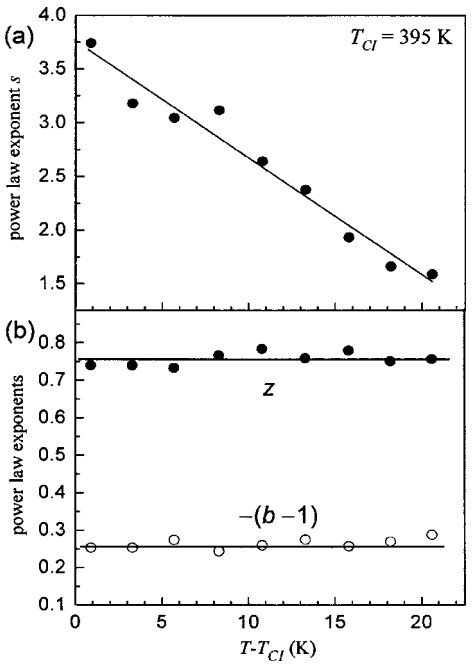


FIG. 3. The results of the fits to the data in Fig. 2 using Eq. (1). (a) Temperature dependence of the short time power law (fast $\beta$ process) exponent $s$. The line through the data is a guide to the eyes. (b) Temperature dependence of the intermediate power law exponent $z$ (filled circles) and von Schweidler power law exponent plotted as $-(b-1)$ (open circles). $z$ and $b$ are independent of $T$. The lines through the points show the average values.

The fitting results for the three power law exponents are displayed in Fig. 3. The short time power law exponent $s$ [Fig. 3(a)] increases with decreasing temperature. Because the short time power law $t^{-s}$ can be observed only over a very limited time range, it is not possible to be certain of its functional form. For supercooled liquids, MCT predicts that the fastest time scale decay is a power law called the fast $\beta$ process.[26,39] It has an exponent that is related to the von Schweidler power law exponent $b$ through a gamma function. However, our observation of the very fast power law exponent does not obey the theoretical relation. What is clear from the data is that the short time dynamics are temperature dependent. The same behavior has also been observed earlier for nematogens.[13]

Figure 3(b) displays the two longer time scale power law exponents from Eq. (1), the intermediate power law ($z$), and von Schweidler power law $-(b-1)$. Both exponents are independent of the temperature within experimental error. Previous OHD-OKE studies on supercooled liquids and rodlike nematogens in the isotropic phase also displayed temperature independent exponents for these two power laws. From Fig. 3(b), the von Schweidler power law exponent $b$ is found to

be 0.74±0.01. For molecular supercooled liquids, $b$ is found to vary from 0.73 to 0.85.[22] For six nematogens in the isotropic phase, $b$ values are all very close to 1.[13,15] The $b$ value of HPT falls into the range of the supercooled liquids. The average value for $z$ is 0.76±0.02 for HPT. For nematogens in the isotropic phase, it was found that $z$ is related to the nematogen structure, with $z$ increasing as the aspect ratio decreases.[14,15] For supercooled liquids, molecules have irregular shapes with small aspect ratios. Values for $z$ vary between 0.79 to 1.0 with no obvious correlation with the molecular geometry.[15] A boundary between normal liquids and nematogens is located at an aspect ratio of 2.5, the value below which theoretical calculation indicates that a nematic phase will no longer exist.[40] A linear extrapolation of $z$ versus the aspect ratio shows that when the aspect ratio grows to ~2.5, the value of $z$ would be 0.85, which falls in the middle of the range observed for supercooled liquids.[14,15] The $z$ value for discotic liquid crystal HPT is slightly below the range of $z$ values observed for supercooled liquids. Simple molecular modeling of an isolated HPT indicates that the molecule is not planar. There is a pair of five carbon side chains on each outer benzenelike ring of the central aromatic portion of the molecule. The chains in a pair are staggered above and below the plane of the aromatic center, that is, one chain is above the plane and one is below. The diameter of the disklike molecule including the chains is ~23 Å. If the thickness is taken to be the distance from the end of one chain that is above the plane to the end of another chain that is below the plane, then it is ~9 Å. (In the columanr phase the spacing between neighboring disks is 3.6 Å,[2] much smaller than the thickness defined here.) The resulting aspect ratio is 2.6. However, this is the opposite of a rodlike nematogen which is long and thin. This structure is short and thick. The $z$ value of 0.76 is somewhat below the values for supercooled liquids and equal within experimental error to the largest value observed for a nematogen, 1-isothiocyanato-(4-propylcyclohexyl) benzene (3-CHBT), which is rodlike with an aspect ratio of 3.3.[15]

The results of fitting the long time exponential decay time $\tau$ are displayed in Fig. 4(a). $\tau$ increases with decreasing temperature and it approximately doubles as $T$ is lowered in the isotropic phase by ~20 K in the vicinity of the *C-I* phase transition. Compared to nematogens in the isotropic phase, the temperature dependence of the exponential long time scale dynamics in HPT is much more gradual, which can be clearly seen in Fig. 4(b). In Fig. 4(b), the exponential time constant of a nematogen in the isotropic phase, 4-(4′-pentylcyclohexyl)-benzonitrile (5PCH),[13] is plotted on the same scale as HPT. For 5PCH, $\tau$ diverges as the *N-I* phase transition is approached from above. This divergence is well explained by the Landau-de Gennes (LdG) theory.[23] In the isotropic phase above but near the *N-I* phase transition, nematogens are orientationally ordered over a length scale defined by correlation length $\xi$. These local structures are referred to pseudonematic domains. Randomization of the domains gives rise to the exponential decays in time domain OHD-OKE experiments. LdG theory predicts that $\xi$ diverges at the second order phase transition temperature $T^*$ as $(T^*/T-T^*)^{1/2}$. The *N-I* phase transition is weakly first order with the result that $T^*$ is slightly below the first order phase transition temperature $T_{NI}$.[23] As $T_{NI}$ is approached from above, $\xi$ grows to a very large value. Consequently, the relaxation time increases dramatically as the pseudonematic domains grow. The divergence in correlation length and relaxation time is a characteristic feature of the continuous (second order) phase transition. Weakly first order phase transitions like *N-I* phase transition can display this feature as well.[23] For the discotic liquid crystal HPT studied here, which forms a hexagonal columnar phase at lower temperatures, no divergence in correlation time is observed in the high temperature isotropic phase as the *C-I* phase transition is approached. The lack of divergence in $\tau$ as the phase transition is approached is consistent with the fact that the *C-I* phase transition is strongly first order as demonstrated by the results of order parameter[4] and differential scanning calorimetry (DSC) measurements.[3]

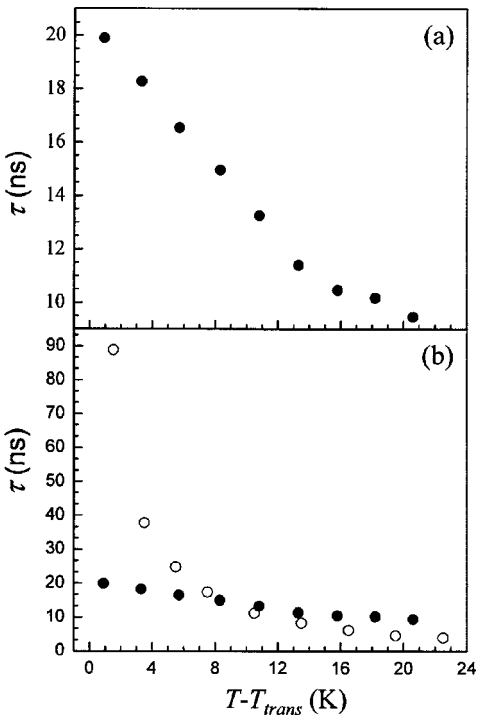


FIG. 4. The long time scale exponential decay time constant $\tau$ as a function of reduced temperature $T$-$T_{\text{trans}}$ for (a) HPT and for (b) HPT (filled circles) and a rodlike nematogen in the isotropic phase 5PCH (open circles). $T_{\text{trans}}$ is the *C-I* phase transition temperature for HPT and the isotropic to nematic phase transition temperature for 5PCH.

For a normal liquid that lacks local structure, the long time scale dynamics are diffusive with temperature dependence primarily determined by the liquid viscosity. The Debye-Stokes-Einstein equation for orientational relaxation is $\tau = V_{\text{eff}}\eta(T)/k_BT$, where $V_{\text{eff}}$ is the effective molecular volume, $\eta(T)$ is the viscosity, and $k_B$ is Boltzmann's constant. Assuming that the viscosity displays an Arrhenius behavior, over the temperature range studied here, the $T$ in the denominator has a negligible influence on the temperature dependence of $\tau$. Figure 5 shows a fit (line) of the natural log of $\tau$ (points) to an Arrhenius-type temperature dependence. The fit yields 63±2 kJ/mol for the activation energy for the viscosity. (The actual viscosities as a function of temperature have not been reported.) It is informative to compare this

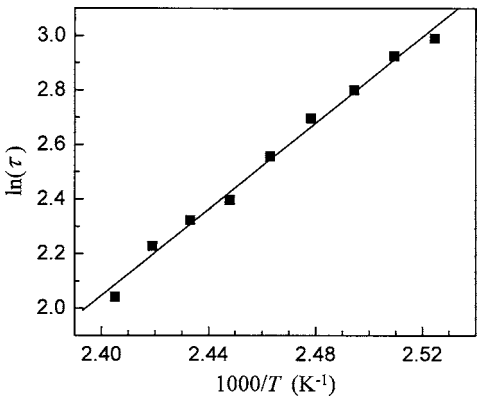


FIG. 5. Arrhenius plot of the long time scale exponential decay time constant $\tau$ of HPT. The activation energy is 63±2 kJ/mol from the slope of the linear fit (line).

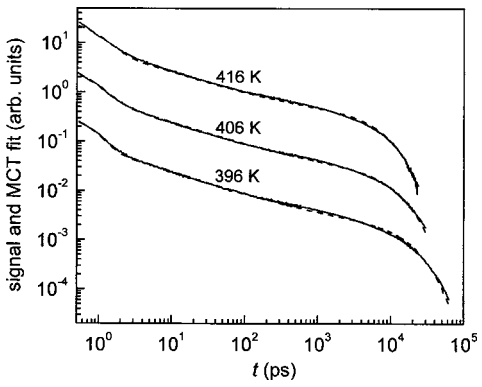


FIG. 6. OHD-OKE data and the MCT calculated curves (dashed curves) using the solutions to Eqs. (2)–(4) on a log plot. Three temperatures are shown: the highest, an intermediate, and the lowest temperature. The curves have been offset along the vertical axis for clarity of presentation.

activation energy to glass forming liquids that are not columnar liquid crystals. Fragile glass forming liquids[41] far from the glass transition temperature $T_g$ have viscosities that display Arrhenius behavior. The activation energies of dibutylphthalate, *ortho*-terphenyl, salol, and glycerol are 41.6 kJ/mol(70 K), 46.3 kJ/mol(90 K), 35 kJ/mol(80 K), and 51 kJ/mol(100 K), respectively. The numbers in parentheses are the number of degrees above $T_g$ at which the determination of the activation energy began. The activation energy for HTP is above all of these although in the same general range. Glycerol is the closest, and it forms a strong hydrogen bond network. However, HTP is substantially larger than the other molecules.

For molecular liquids that display complex dynamical profiles, MCT (Ref. 26) has proven useful for describing the relaxation processes over the entire time window without arbitrary separations of time scales. Previously MCT was applied to time domain OHD-OKE experiments on several supercooled liquids at temperatures above and relatively close to the critical temperature $T_c$. The data were found to obey certain scaling relations predicted from asymptotic solutions of MCT equations.[22] The numerical solutions of a two-correlator schematic MCT model[28,42] were able to successfully reproduce the OHD-OKE decay curves over a wide time window spanning subpicoseconds to hundreds of nanoseconds.[20,28] The MCT model is also applicable for a normal liquid above its melting point.[43] The OHD-OKE data for HPT infer that it behaves like a normal liquid above a first order phase transition. The temperature range studied here is substantially higher than $T_c$, which is typically $\sim 1.2T_g$. Here the applicability of the two-correlator schematic MCT model is investigated for HPT. The MCT schematic model is based on the Sjögren model,[42] which involves two correlators, one for density and one for orientation,[20,28] the experimental observable of OHD-OKE spectroscopy. The equations for both correlators have the form of a damped harmonic oscillator with a memory term. The memory term accounts for "caging" of a given molecule by surrounding molecules. Caging prevents the complete relaxation of density and orientational correlations on short time scales. Relaxation of the cage permits the final long time scale complete diffusive randomization of the system. On short time scales, the memory effects associated with caging produce nonexponential dynamics.

In the following, $\phi_1$ is the density correlation function and $\phi_2$ is the orientation correlation function. The equations for the coupled density and orientational dynamics are given by

$$\ddot{\phi}_i(t) = -\Omega_i^2 \phi_i(t) - \mu_i \dot{\phi}_i(t) - \Omega_i^2 \int_0^t dt' m_i(t-t') \dot{\phi}_i(t'), \quad i = 1,2, \tag{2}$$

where $\Omega_{1,2}$ are the characteristic frequencies and $\mu_{1,2}$ are the damping constants for the density and orientation correlators, respectively. The memory functions inside the integrals account for the caging effects. The density relaxation is complicated by correlations in the local density that inhibits relaxation. This caging becomes more pronounced as the temperature is lowered. The memory function uses an $F_{12}$ model, that is, it contains a term that is linear in the correlation function and a term that is quadratic in the correlation function [see Eq. (3) below].[26] The experimental observable correlation function is coupled to the density correlator, which possesses the relevant singular behavior as the mode coupling transition is approached. Coupling the orientational correlation function to the density correlation function builds memory into the orientational relaxation. The memory kernels are given by

$$m_1(t) = v_1 \phi_1(t) + v_2 \phi_1^2(t), \tag{3}$$

$$m_2(t) = k \phi_2(t) \phi_1(t), \tag{4}$$

where $\nu_1$ and $\nu_2$ are the amplitudes of the two terms in the density memory kernel and $k$ is the translation-rotation coupling constant. The initial conditions are $\phi_{1,2}(0)=1$ and $\dot{\phi}_{1,2}(0)=0$.

There are a large number of parameters involved in this calculation. For supercooled liquids, the characteristic frequencies are on the order of terahertz.[20,32,38] It was found previously that the nature of the results is not sensitive to the choice of $\Omega_1$ and $\Omega_2$ so long as they are in the terahertz range. To reduce the complexity and be consistent with the

TABLE I. Results of MCT fits.

| $T$ (K) | $\kappa$ | $\nu_1$ | $\nu_2$ |
|---|---|---|---|
| 416 | 101.2 | 0.90 | 0.03±0.03 |
| 406 | 111.9 | 0.93 | 0.02±0.02 |
| 396 | 138.3 | 0.94 | 0.06±0.04 |

values used earlier for supercooled liquids, we fixed $\Omega_1 = 1$ THz and $\Omega_2 = 0.5$ THz at all temperatures.[20,38] The theoretical curves for comparison to the experimental data were calculated as the time derivative of $\phi_2(t)$ obtained from the solutions of Eqs. (2)–(4). A downhill simplex algorithm was used to optimize the parameters to obtain a best match to the experimental data. Initially, the other five parameters were allowed to vary. It was found that $\mu_1$ and $\mu_2$ had almost no temperature dependence. Therefore, they were fixed at the average values found in the initial fits, that is, $\mu_1 = 6.3$ THz and $\mu_2 = 45.1$ THz. With these values fixed, the data were again fit, and the quality of the fits was not degraded.

Figure 6 illustrates the efficacy of MCT for describing HPT dynamics in the isotropic phase. Three temperatures are shown: the highest, the lowest, and an intermediate temperature. For all three temperatures, MCT does a reasonable job of reproducing the data from less than picosecond to a few tens of nanoseconds. The parameters obtained from the fits are given in Table I. $\nu_2$ is very close to zero. This is consistent with recent results on a supercool liquid, *N*-propyl-3-methylpyridinium bis(trifluoromethylsulfonyl)-imide, which was studied from far above $T_c$ down to $T_c$.[38] Far above $T_c$, $\nu_2$ was found to be approximately zero but increasing as $T$ was decreased. In that same study, $\nu_1$ was essentially constant with a value of 0.97. Values of $\nu_1$ of ~0.9 were found for two other supercooled liquids, acetylsalicylic acid and dibutylphthalate, to which the MCT treatment used here was applied. However, these liquids were not studied at sufficiently high temperature to see if $\nu_2$ went to zero. Therefore, the values of $\nu_1$ and $\nu_2$ observed here are consistent with liquids that do not go through a first order phase transition. Neither $\nu_1$ nor $\nu_2$ displays substantial temperature dependences over the limited range of temperatures studied. However, the rotation-translation coupling constant, $\kappa$, does show a significant change. As the temperature is decreased, the rotation-translation coupling increases. The lowest temperature is only 1 K above the first order phase transition. Although $\kappa$ increases, its behavior is in sharp contrast to the behavior of nematogens in the isotropic phase. It was found that in nematogen systems studied, $1/\kappa$ tends to zero at $T^*$ as the second order phase transition is approached from above.[29] The discotic system studied here shows no indication of divergent behavior as the phase transition is approached. Rather, it behaves like a normal liquid that is far above $T_g$ and $T_c$.

## IV. CONCLUDING REMARKS

We have presented OHD-OKE data on a discotic liquid crystal HPT in the isotropic phase at temperature of ~1–20 K above the isotropic to columnar phase transition. The OHD-OKE decay curves can be fit very successfully using a phenomenological function that has been proven to work well for supercooled liquids and nematogens in the isotropic phase. An intermediate power law $t^{-0.76\pm0.02}$ and a von Schweidler power law $t^{-0.26\pm0.01}$ are observed at short to intermediate times, and the long time scale decay is a single exponential decay. The intermediate power law exponent is close to the boundary between those found for supercooled liquids and nematogens in the isotropic phase, while the von Schweidler power law exponent is undoubtedly different from nematogens in the isotropic phase and falls in the range of supercooled liquids. In spite of the fact that HPT is very far above $T_g$ (~200 K) and close to a first order phase transition, its dynamical characteristics closely resemble those of supercooled liquids. In contrast to nematogens in the isotropic phase, the long time exponential decays show Arrhenius-type temperature dependence and no divergence in the decay time is observed as the *C-I* phase transition is approached from above.

We have also analyzed the HPT data using a schematic MCT model, the Sjögren model.[20,28,42] This model has been shown to be able to reproduce the OHD-OKE data for molecular glass forming liquids over a broad temperature range from $T_c$ to well above $T_c$.[20,28,43] The dynamical similarity between supercooled liquids and nematogens in the isotropic phase inspired the expansion of the schematic model to describe the dynamics of nematogens in the isotropic phase. A MCT model, modified by incorporating LdG like terms into the Sjögren model was able to reproduce the OHD-OKE data of nematogens in the isotropic phase over the full range of times and temperatures.[29] The fact that the original MCT supercooled liquid model can fit the HPT data without any additions to account for the approach to the *C-I* phase transition confirms that HPT in the isotropic phase behaves like a normal liquid apparently without local structures that exist in the isotropic phase of nematogens.

## ACKNOWLEDGMENT

This work was supported by the National Science Foundation (DMR-0332692).

[1] S. Chandrasekhar, B. K. Sadashiva, and K. A. Suresh, Pramana **9**, 471 (1977).
[2] A. M. Levelut, J. Phys. (Paris), Lett. **40**, 81 (1979).
[3] M. T. Allen, K. D. M. Harris, B. M. Kariuki, N. Kumari, J. A. Preece, S. Diele, D. Lose, T. Hegmann, and C. Tschierske, Liq. Cryst. **27**, 689 (2000).
[4] J. K. Vij and A. Kocot, Mol. Cryst. Liq. Cryst. **397**, 231 (2003).
[5] J. D. E. Dantras, C. Lacabanne, L. Laffont, J. M. Tarascon, S. Archambeau, I. Seguy, P. Destruel, H. Bockd, and S. Fouetd, Phys. Chem. Chem. Phys. **6**, 4146 (2004).
[6] H. Groothues, F. Kremer, D. M. Collard, and C. P. Lillya, Liq. Cryst. **18**, 117 (1995).
[7] F. M. Mulder, J. Stride, S. J. Picken, P. H. J. Kouwer, M. P. d. Haas, L. D. A. Siebbeles, and G. J. Kearley, J. Am. Chem. Soc. **125**, 3860 (2003).
[8] G. Cinacchi, R. Colle, and A. Tani, J. Phys. Chem. B **108**, 7969 (2004).
[9] X. Shen, R. Y. Donga, N. Boden, R. J. Bushby, P. S. Martin, and A. Wood, J. Chem. Phys. **108**, 4324 (1998).
[10] M. Vilfan, G. Lahajnar, V. Rutar, R. Blinc, B. Topic, A. Zann, and J. C. Dubois, J. Chem. Phys. **75**, 5250 (1981).
[11] S. V. Dvinskikh, I. Furó, H. Zimmermann, and A. Maliniak, Phys. Rev. E **65**, 050702 (2002).
[12] R. Y. Dong, D. Goldfarb, M. E. Moseley, Z. Luz, and H. Zimmermann, J. Phys. Chem. **88**, 3148 (1984).

[13] J. Li, I. Wang, and M. D. Fayer, J. Chem. Phys. **124**, 044906 (2006).
[14] H. Cang, J. Li, and M. D. Fayer, Chem. Phys. Lett. **366**, 82 (2002).
[15] H. Cang, J. Li, V. N. Novikov, and M. D. Fayer, J. Chem. Phys. **118**, 9303 (2003).
[16] S. D. Gottke, D. D. Brace, H. Cang, B. Bagchi, and M. D. Fayer, J. Chem. Phys. **116**, 360 (2002).
[17] S. D. Gottke, H. Cang, B. Bagchi, and M. D. Fayer, J. Chem. Phys. **116**, 6339 (2002).
[18] D. Brace, S. D. Gottke, H. Cang, and M. D. Fayer, J. Chem. Phys. **116**, 1598 (2002).
[19] S. D. Gottke, D. D. Brace, G. Hinze, and M. D. Fayer, J. Phys. Chem. B **105**, 238 (2001).
[20] H. Cang, J. Li, H. C. Andersen, and M. D. Fayer, J. Chem. Phys. **123**, 064508 (2005).
[21] H. Cang, V. N. Novikov, and M. D. Fayer, Phys. Rev. Lett. **90**, 197401 (2003).
[22] H. Cang, V. N. Novikov, and M. D. Fayer, J. Chem. Phys. **118**, 2800 (2003).
[23] P. G. de Gennes, *The Physics of Liquid Crystals* (Clarendon, Oxford, 1974).
[24] M. Ebert, D. A. Jungbauer, R. Kleppinger, J. H. Wendorff, B. Kohne, and K. Praefcke, Liq. Cryst. **4**, 53 (1989).
[25] D. Chakrabarti, P. P. Jose, S. Chakrabarty, and B. Bagchi, Phys. Rev. Lett. **95**, 197801 (2005).
[26] W. Götze, *Liquids, Freezing and Glass Transition* (Elsevier Science, Amsterdam, 1989).
[27] B. Bagchi and S. Bhattacharyya, Adv. Chem. Phys. **116**, 67 (2001).
[28] W. Götze and M. Sperl, Phys. Rev. Lett. **92**, 105701 (2004).
[29] J. Li, H. Cang, H. C. Andersen, and M. D. Fayer, J. Chem. Phys. **124**, 014902 (2006).
[30] D. McMorrow, W. T. Lotshaw, and G. A. Kenney-Wallace, IEEE J. Quantum Electron. **24**, 443 (1988).
[31] G. Hinze, D. Brace, S. D. Gottke, and M. D. Fayer, Phys. Rev. Lett. **84**, 2437 (2000).
[32] P. Boon and S. Yip, *Molecular Hydrodynamics* (McGraw-Hill, New York, 1980).
[33] Y. Kai, S. Kinoshita, M. Yamaguchi, and T. Yagi, J. Mol. Liq. **65/66**, 413 (1995).
[34] Y. X. Yan and K. A. Nelson, J. Chem. Phys. **87**, 6240 (1987).
[35] Y. X. Yan and K. A. Nelson, J. Chem. Phys. **87**, 6257 (1987).
[36] F. W. Deeg, J. J. Stankus, S. R. Greenfield, V. J. Newell, and M. D. Fayer, J. Chem. Phys. **90**, 6893 (1989).
[37] Y.-X Yan, L.-T. Cheng, and K. A. Nelson, in *Advances in Nonlinear Spectroscopy*, Advances in Spectroscopy Series 16, edited by R. J. H. Clark and R. E. Hester (Wiley, New York, 1987), Vol. 16, p. 299.
[38] J. Li, I. Wang, K. Fruchey, and M. D. Fayer, J. Phys. Chem. A **110**, 10384 (2006).
[39] G. Hinze, D. D. Brace, S. D. Gottke, and M. D. Fayer, J. Chem. Phys. **113**, 3723 (2000).
[40] M. Letz, R. Schilling, and A. Latz, Phys. Rev. E **62**, 5173 (2000).
[41] C. A. Angell, J. Phys. Chem. Solids **49**, 863 (1988).
[42] L. Sjögren, Phys. Rev. A **33**, 1254 (1986).
[43] M. Ricci, S. Wiebel, P. Bartolini, A. Taschin, and R. Torre, Philos. Mag. **84**, 1491 (2004).